Fourier Acceleration of SU(3) Pure Gauge Theory at Weak Coupling

Yikai Huo, Norman Christ

August 1st, 2023

Overview

Critical Slowing Down

Critical Slowing Down

When the lattice spacing becomes smaller, the high-energy modes will need a smaller time step to carry out precise integration. However, this will result in more time steps to evolve the long-distance modes.

Solution

- Classify different modes.
- Use Fourier acceleration to achieve the same evolution velocity for each mode.

Analogy

Imagine a set of harmonic oscillator

$$H = \sum_{i=1}^{N} \frac{p_i^2}{2m_i} + \frac{1}{2} k_i x_i^2 \tag{1}$$

If mass term m does not depend on i, we are choosing the momenta from the distribution $e^{-p_i^2/2m}$ each mode will have the same velocity. Modes with larger ω_i need a shorter time step than the modes of smaller ω_i. By imposing $m_i \propto k_i$, we can make ω_i the same for each mode and hence remove critical slowing down.

Gauge-Fixing Action

Action

Our action consists of two parts: one is the Wilson action, the other one is soft gauge-fixing term.

$$S = S_W + S_{GF} \tag{2}$$

Soft Gauge-Fixing Term

The soft gauge-fixing action refers to *D. Zwanziger, 1990*, *C. Parrinello, 1990* and *S. P. Fachin, 1993*. It consists of a gauge-fixing term

$$S_{GF1}[U] = -\frac{1}{3}\beta M^2 \sum_{n,\mu} \mathrm{ReTr}[U_\mu] \tag{3}$$

and its corresponding Faddeev-Popov term.

$$S_{GF2}[U] = \ln \int \mathrm{d}g \exp\left(\frac{1}{3}\beta M^2 \sum_{n,\mu} \mathrm{ReTr}[U_\mu^g]\right) \tag{4}$$

Gauge-Fixing Action

Finite-Volume Weak-coupling Expansion

$$S_{\mathrm{FV}}[U] = \frac{\beta}{12}\sum_{n}\Bigg(M^2\left(\nabla_\mu A_\mu\right)\frac{1}{\nabla^2}\left(\nabla_\nu A_\nu\right) + \frac{1}{2}\sum_{\mu,\nu}\left(A_\mu(n) + A_\nu(n+\hat{\mu}) - A_\nu(n) - A_\mu(n+\hat{\nu})\right)^2\Bigg) \tag{5}$$

The blue term is expansion of Wilson action and the red term is expansion of gauge-fixing term.

The algorithm is presented by Y. Zhao during Lattice 2018 (10.22323/1.334.0026). The numerical result with frozen boundary lattice is presented by A. Sheta during Lattice 2021 (10.22323/1.396.0084).

Fixed Boundary Condition

We impose a fixed boundary condition on our lattice. It requires the gauge field vanishes at the edge of the lattice.

$$\begin{cases} U_\mu(n)|_{n_\rho=0} = U_\mu(n)|_{n_\rho=N_\rho} = 1 \\ A_\mu(n)|_{n_\rho=0} = A_\mu(n)|_{n_\rho=N_\rho} = 0 \end{cases} \quad \text{for} \quad \rho \neq \mu. \tag{6}$$

With this boundary condition, **we can break the pure-gauge Z_3 symmetry, eliminating tunneling between degenerate Z_3 phases**.

Here it may be convenient to refer to the figure which shows a 2-dimensional lattice with $N_0 = N_1 = 4$. The red links are free while the blue links are fixed to unit matrices.

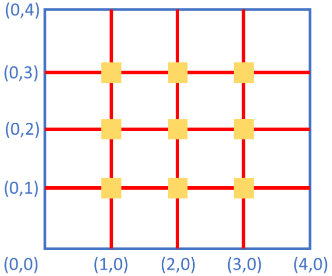

Position Dependence

With these new boundary conditions, the modes are no longer plane waves. We need to specialize the modes $A_\mu(k,n)$ to fulfill the fixed boundary condition which are combinations of those plane waves. Since the gauge field vanishes at the edge of the lattice, we can easily deduce that position-dependence of the μ-component of a mode in the three directions different from μ.

$$A_\mu(k,n) \propto \prod_{\substack{\rho=0 \\ \rho\neq\mu}}^{3} \sqrt{\frac{2}{N_\rho}} \sin(k_\rho n_\rho) \tag{7}$$

Here, $k = \frac{\pi}{N}\ell$, the integer ℓ_ρ obeys $1 \leq \ell_\rho \leq N_\rho - 1$.

Longitudinal Mode

By evaluating the gauge transformation on the zero field generated by the following $\Lambda(n,k)$, we can construct a zero mode of the Wilson action, which we call the longitudinal mode $A_{L,\mu}(k,n)$ with polarization vector $\varepsilon_{L,\mu}(k) = \sin\left(\frac{k_\mu}{2}\right)$.

$$\begin{aligned} \Lambda(n,k) &= \prod_{\rho=0}^{3} \sin(k_\rho n_\rho) \\ A_{L,\mu}(k,n) &= \sin\left(\frac{k_\mu}{2}\right) \cos\left(k_\mu\left(n_\mu + \frac{1}{2}\right)\right) \prod_{\substack{\rho=0 \\ \rho\neq\mu}}^{3} \sin(k_\rho n_\rho) \end{aligned} \tag{8}$$

Here, $k = \frac{\pi}{N}\ell$, the integer ℓ_μ obeys $0 \leq \ell_\mu \leq N_\mu - 1$ and the integer ℓ_ρ obeys $1 \leq \ell_\rho \leq N_\rho - 1$

Transverse Modes

Since we have determined the longitudinal mode, the remaining three transverse modes $A_{T_i,\mu}(k,n)$, for $1 \le i \le 3$ can be constructed from three transverse polarization vectors $\varepsilon_{T_i,\mu}(k)$ which are orthogonal to $\varepsilon_{L,\mu}(k)$ and each other.

$$\begin{aligned} &\sum_{\rho=0}^{3} \varepsilon_{T_i,\rho}(k)\varepsilon_{T_j,\rho}(k) = \delta_{ij} \\ &\sum_{\rho=0}^{3} \varepsilon_{T_i,\rho}(k)\varepsilon_{L,\rho}(k) = 0, \text{ for } 1 \le i \le 3. \end{aligned} \tag{9}$$

These transverse modes all have the same eigenvalue of Wilson action.

$$\lambda_T = 4\sum_{\mu=0}^{3} \sin^2\left(\frac{k_\mu}{2}\right). \tag{10}$$

Modes

Finally, we get a set of eigenmodes of Wilson action.

$$A_{X,\mu}(k) = \varepsilon_{X,\mu}\sqrt{\frac{2}{N_\mu}}\cos\left(k_\mu\left(n_\mu+\frac{1}{2}\right)\right)\prod_{\substack{\rho=0\\ \rho\neq\mu}}^{3}\sqrt{\frac{2}{N_\rho}}\sin(k_\rho n_\rho) \tag{11}$$

Here, $X = L, T_1, T_2, T_3$, meaning different modes, $\varepsilon_{X,\mu}$ stands for the polarization, $k = \frac{\pi}{N}\ell$, the integer ℓ_μ obeys $0 \leq \ell_\mu \leq N_\mu - 1$ and the integer ℓ_ρ obeys $1 \leq \ell_\rho \leq N_\rho - 1$.

We need to use discrete sine and cosine transformation, instead of FFT, to transform the field between position space and wave number space.

$$\begin{aligned}\widetilde{A}_\mu(k) &= \sum_{n_\mu=0}^{N_\mu-1}\sum_{\substack{n_\rho=1\\ \rho\neq\mu}}^{N_\rho-1} A_\mu(n)\psi(n,\ell)_\mu \\ \psi(n,\ell)_\mu &= \sqrt{\frac{2}{N_\mu}}\cos\left(\frac{\pi}{N_\mu}\ell_\mu\left(n_\mu+\frac{1}{2}\right)\right)\prod_{\substack{\rho=0\\ \rho\neq\mu}}^{3}\sqrt{\frac{2}{N_\rho}}\sin(\frac{\pi}{N_\rho}\ell_\rho n_\rho)\end{aligned} \tag{12}$$

Action in Momentum Space

Rewrite Action in the Weak Coupling Limit

We can rewrite the weak coupling expansion with the modes we find

$$S[U] \approx \frac{\beta}{12} \sum_{k,\mu,\nu} \widetilde{A}_\mu(k) \left(4 \left(\sum_{\mu=0}^{3} \sin^2 \left(\frac{k_\mu}{2} \right) \right) \mathrm{P}^T_{\mu\nu} + M^2 \mathrm{P}^L_{\mu\nu} \right) \widetilde{A}_\nu(k). \tag{13}$$

Projection Operators

$\mathrm{P}^T_{\mu\nu}$ and $\mathrm{P}^L_{\mu\nu}$ are corresponding projection operator of transverse modes and longitudinal modes.

$$\begin{aligned} \mathrm{P}^T_{\mu\nu} &= \delta_{\mu\nu} - \frac{\sin\left(\frac{k_\mu}{2}\right)\sin\left(\frac{k_\nu}{2}\right)}{\sum_{\mu=0}^{3} \sin^2(\frac{k_\mu}{2})} \\ \mathrm{P}^L_{\mu\nu} &= \frac{\sin\left(\frac{k_\mu}{2}\right)\sin\left(\frac{k_\nu}{2}\right)}{\sum_{\mu=0}^{3} \sin^2(\frac{k_\mu}{2})} \end{aligned} \tag{14}$$

Fourier Acceleration

We can construct the following kinetic term to implement Fourier acceleration where the coefficients of conjugate momenta to be the inverse of the coefficients of gauge fields in the weak coupling limit.

$$
\begin{aligned}
H_p =& \sum_k \mathrm{Tr}\left(\widetilde{p}_\mu(k) D^{\mu\nu} \widetilde{p}_\nu(k)\right) \\
D^{\mu\nu} =& \frac{1}{4\left(\sum_{\mu=0}^{3} \sin^2\left(\frac{k_\mu}{2}\right)\right)} \mathrm{P}^T_{\mu\nu} + \frac{1}{M^2} \mathrm{P}^L_{\mu\nu}
\end{aligned}
\tag{15}
$$

With this kinetic term, we can obtain the same frequency for all modes.

$$
\begin{aligned}
H =& S[U] + H_p \\
\approx& \frac{1}{2} \sum_{k,\mu} \frac{\left(\widetilde{p}^T_\mu(k)\right)^2}{4\left(\sum_{\mu=0}^{3} \sin^2\left(\frac{k_\mu}{2}\right)\right)} + \frac{1}{2} \sum_{k,\mu} 4\left(\sum_{\mu=0}^{3} \sin^2\left(\frac{k_\mu}{2}\right)\right)\left(\widetilde{A}^T_\mu(k)\right)^2 \\
&+ \frac{1}{2} \sum_{k,\mu} \frac{\left(\widetilde{p}^L_\mu(k)\right)^2}{M^2} + \frac{1}{2} \sum_{k,\mu} M^2 \left(\widetilde{A}^L_\mu(k)\right)^2
\end{aligned}
\tag{16}
$$

Hybrid Monte Carlo

We first generate independent, Gaussian-distributed random numbers $\eta(\ell)_\mu$. The initial conjugate momenta $p(\ell)_\mu$ are then obtained.

$$\widetilde{p}(\ell)_\mu\bigg|_{\tau=0} = \left(\sqrt{4\left(\sum_{\mu=0}^{3}\sin^2\left(\frac{k_\mu}{2}\right)\right)}\mathrm{P}^T_{\mu\nu} + M\mathrm{P}^L_{\mu\nu}\right)\eta(\ell)_\nu. \tag{17}$$

Then we do the leapfrog integration with the following Equation of Motion.

$$\begin{aligned}\dot{A}_\mu(n) &= \sum_{k_\mu=0}^{N_\mu-1}\sum_{\substack{k_\rho=1\\ \rho\neq\mu}}^{N_\rho-1}\psi(n,\ell)_\mu D^{\mu\nu}\widetilde{p}_\nu(\ell)\\ \dot{p}_\mu(n) &= -\frac{\partial S[e^{i\omega^a\lambda^a}U(n)_\mu]}{\partial\omega^a}\bigg|_{\omega^a=0}\end{aligned} \tag{18}$$

Periods of Different Modes with Difference Kinetic Terms

The following plots show the evolution of real parts of 4 modes of the vector potential $A_\mu = \ln U_\mu$ on a 16^4 lattice with the $\beta = 100,\ M = 3.0$ soft gauge-fixing action.

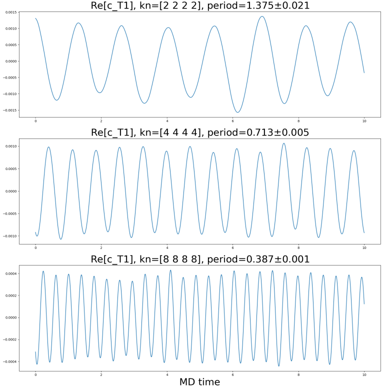

Figure: Original Kinetic Term

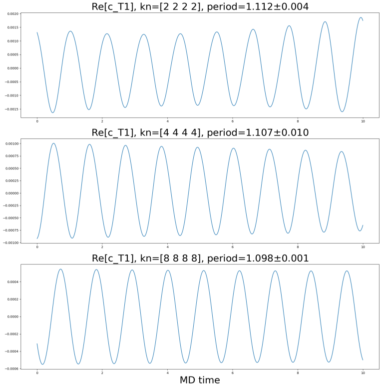

Figure: Fourier Acceleration Kinetic Term

Current Test Result

In order to show the acceleration effect in the generation of independent gauge configurations, we do both original HMC simulations and GFFA simulations on two different volumes' lattices, 8^4 and 16^4, at $\beta = 10$, and compare integrated auto-correlation times of plaquette values U_P.

Integrated Autocorrelation Times

$$\tau_{int} = \frac{1}{2} + \sum_{\Delta=1}^{\Delta_{cut}} C(\Delta)$$
$$C(\Delta) = \left\langle \frac{(U_P(t) - \bar{U}_P)(U_P(t+\Delta) - \bar{U}_P)}{\sigma^2} \right\rangle_t \tag{19}$$

Here, $\bar{U}_P$ is the average plaquette value and σ is the standard deviation.

Current Test Result: Plaquette Correlation Plot 8^4

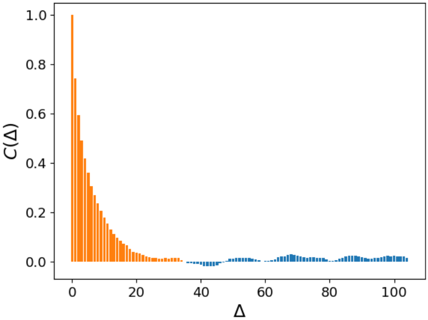

Figure: $C(\Delta)$ Pure HMC

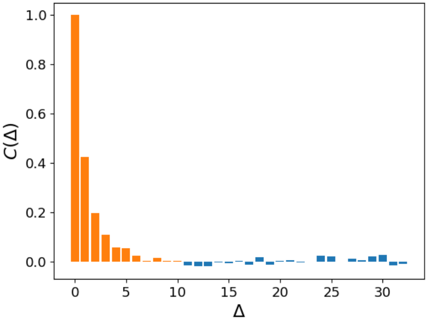

Figure: $C(\Delta)$ GFFA

Current Test Result: Plaquette Correlation Plot 16^4

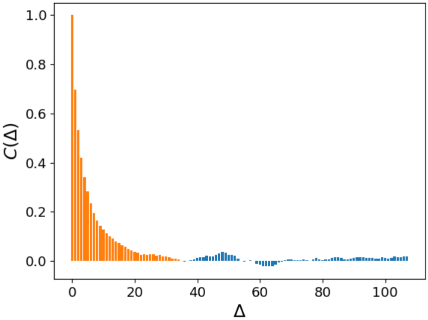

Figure: $C(\Delta)$ Pure HMC

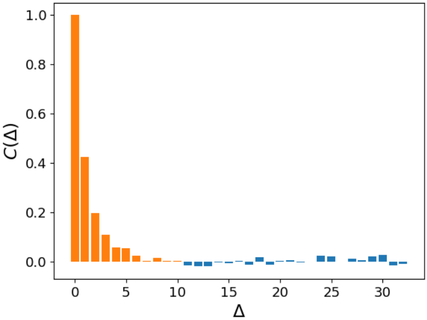

Figure: $C(\Delta)$ GFFA

Current Test Result-Summary

Pure HMC

β	size	traj num	traj L	MDsteps	plaquette	plaq τ_{int}
10	8^4	19940	0.6	24	$0.85094(81)$	5.38(35)
10	16^4	19900	0.6	64	$0.81900(22)$	4.64(33)

GFFA HMC

β	size	M	traj num	traj L	MDsteps	plaquette	plaq τ_{int}
10	8^4	3.0	3924	0.6	48	$0.85090(84)$	1.22(10)
10	16^4	3.0	2184	0.6	64	$0.81903(23)$	1.36(18)

GFFA achieves $4\times$ factor acceleration

Outlook

- Calculate Wilson Flow variables to further test the algorithm's acceleration efficiency.
- Generate configurations with smaller β to search for a practical lower boundary of the algorithm.
- Implement algorithm on large-volume lattice by dividing large lattice into small volumes and applying Fourier acceleration on independent sub-volumes in a checkerboard fashion.
- Long-term goal: Add fermion determinants and test how efficiently the algorithm can reduce critical slowing down with dynamical fermions.